Acoustic Characterization of the NASA Langley 14- by 22-Foot Subsonic Tunnel using a Phased Array

Mary L. Houston,[1] Colin M. Stutz,[2] Nikolas S. Zawodny,[3] Kyle A. Pascioni,[4]
NASA Langley Research Center, 2 North Dryden Street, Hampton, VA 23681

ABSTRACT

A characterization test was conducted in the NASA Langley Research Center 14- by 22-Foot Subsonic Tunnel to assess recent acoustic modifications in the facility. Test section reflectivity, background noise and shear layer effects were evaluated by taking measurements of known noise sources. Both conventional speakers and a high-pressure air source were employed as noise generation mechanisms. These were mounted to a pole or fairing at a consistent location in the test section. The source waveforms were used to represent the expected frequency content of scaled Urban Air Mobility vehicles. Acoustic measurements were taken using two unique microphone arrays placed outside the core flow, one of which was a 54-element streamwise-traversing phased array. The other was an 11-element linear tower array. The applicability of phased array acoustic beamforming techniques to mitigate shear layer effects and reject background noise is presented. Additionally, beamforming results are compared to results from single-microphone processing techniques. Flow speeds investigated ranged from Mach 0.00 (static) to Mach 0.12. The tunnel has been partially acoustically treated but still exhibits flow noise, reducing the signal-to-noise ratio of the source under investigation. Conventional beamforming was able to capture high frequency content passing through the shear layer better than single microphone measurements. CLEAN deconvolution improves source mapping at low frequencies.

1. INTRODUCTION

The emergence of the Urban Air Mobility (UAM) sector has made the impact of integrating a greater number of aircraft into the urban environment increasingly relevant. One such impact is the sound generated aerodynamically by these vehicles. These vehicles may be quieter than traditional

[1]Mary.L.Houston@nasa.gov

[2]Colin.M.Stutz@nasa.gov

[3]Nikolas.S.Zawodny@nasa.gov

[4]Kyle.A.Pascioni@nasa.gov

rotorcraft or fixed-wing vehicles, which presents a challenge to aeroacousticians who, therefore, may have to work with a lower signal-to-noise ratio (SNR). Although the vehicles may be quieter at the source, their anticipated prevalence and proximity to communities make understanding their noise characteristics important. Scaled wind-tunnel tests are an important step in understanding these noise sources. Larger test models are preferable both because they can more closely match the anticipated flight conditions of full-scale vehicles, and because a larger test model allows for more sophisticated instrumentation. This makes NASA Langley's 14- by 22-Foot Subsonic Tunnel (the 14x22) a desirable testing facility. The 14x22 was not designed as a quiet tunnel, although some acoustic treatment was built into the walls to reduce noise levels in the control rooms. Over the years more extensive acoustic modifications have been applied to allow for the collection of acoustic data [1–4].

Recent acoustic tests in the 14x22 have included three airframe noise- and propulsion airframe aeroacoustics-focused entries: the semispan High-Lift Common Research Model (CRM) [1, 2]; a semispan Gulfstream model [5] and a full-span Hybrid Wing Body (HWB) aircraft model [3, 4, 6]. There was also a model tiltrotor entry [7]. The airframe noise entries focused on higher-frequency broadband phenomena between 1 and 80 kHz, where tunnel background noise is relatively low. The tiltrotor test included frequencies of interest below 1 kHz, but these were high-amplitude, often impulsive, tonal noise sources related to the blade passage frequency (BPF), which stood out against the background noise or could be isolated from background noise through periodic averaging.

To investigate acoustic characteristics of scaled UAM models, signals between approximately 100 Hz and 10 kHz must be measured. Some components of the measured noise will be periodic, or at least tied to the BPF, allowing periodic averaging to improve signal quality, but much of the noise is expected to be broadband and stochastic in nature. In the frequency range of interest, this stochastic noise will likely blend into facility background noise. The use of a phased microphone array and acoustic beamforming can help isolate a source from background noise, particularly at higher flow speeds.

2. EXPERIMENTAL SETUP

2.1. Test Facility

The experimental data were collected in the 14x22 operating in the open-jet configuration. Dimensions of the tunnel test section are 14.50 feet high, 21.75 feet wide and 50 feet long. It is a closed-circuit atmospheric wind tunnel that can operate in closed- or open-jet configuration. In the open-jet configuration, the tunnel can operate at flow speeds from Mach 0.02 to Mach 0.26. For this test, flow speeds up to Mach 0.2 were reached; however, due to concerns about shear layer buffeting shaking the phased array, only speeds up to Mach 0.12 were reached routinely.

The 14x22 was not constructed to be an acoustic tunnel; however, it has been acoustically treated. Many of the walls of the open-jet test section have been treated with perforated metal panels backed by fiberglass insulation to reduce reflections and also to prevent excess sound from the test section from entering the control room and other parts of the building. Six-inch, 0.5 lb/ft^3 density, melamine foam wedges have been permanently added to the section of the north wall, directly behind the phased array. The same acoustic wedges were installed on the ceiling for the open-jet configuration. In the open-jet configuration, the perforated sheet metal panels and acoustic wedges are largely out of the flow, and therefore are not a source of scrubbing noise. However, the test section floor is not completely removed, so smooth-topped treatments had to be designed for the floor, as shown in Figure 1. Metal

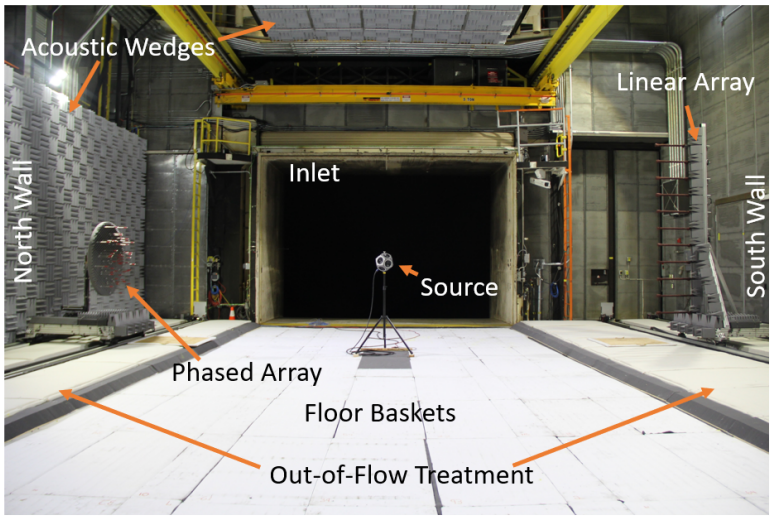

Figure 1: 14x22 test section in open-jet/acoustic configuration. [Source: NASA]

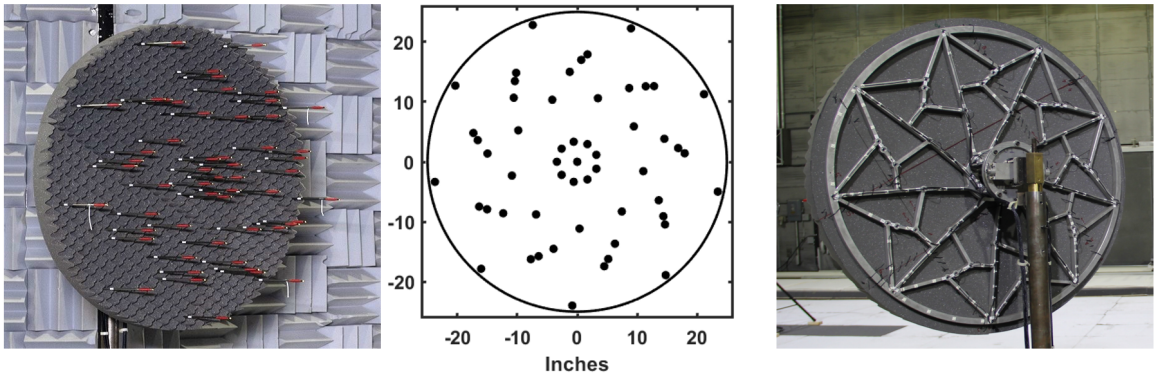

Figure 2: Phased array front, microphone pattern and back. [Source: NASA]

baskets with a depth of two feet (floor baskets) containing layers of low (2 lb/ft^3) and high (6 lb/ft^3) density acoustic foam have been employed. Various design iterations of the upper layer of these baskets (basket tops) have been deployed in past acoustic tests. In the present test, the basket tops were redesigned to reduce reflectivity without increasing scrubbing noise. The design and testing of these modifications will be summarized in [8]. Acoustic treatments were also applied to the areas of the floor between the test section and the walls. These so-called "out-of-flow" treatments were comprised of wooden frames filled with 6-inch fiberglass insulation and covered with cloth.

2.2. Microphone Arrays

The present analysis focuses on the performance and characteristics of the phased microphone array (phased array). As seen in Figure 2, the phased array was comprised of 54 Brüel and Kjær (B&K) Type 4958 1/4-inch microphones. All array microphones were sampled at 65,536 samples per second to allow adequate frequency resolution up to 25 kHz. The innermost 45 elements were arranged in nine arms of five microphones and utilize a reverse-log distribution [9]. This array layout was chosen to minimize the 3-dB beamwidth while maintaining peak sidelobe levels at least 10 dB below the main lobe over a range of 1 to 16 kHz. Additionally, an outer ring of nine microphones at a diameter of 48 inches was added to improve low frequency resolution. There was also a B&K Type 4954

microphone placed in the center of the array to be used as reference, and so was not included in beamforming calculations. To illustrate the ability of the array to suppress sidelobe levels, Figure 3 shows simulated point spread functions (PSFs) for the array at 1, 5, 10 and 20 kHz for the same scan plane. For these figures, each array response is depicted with two dynamic ranges, 10 dB and 20 dB. It can be seen that sidelobes are not within 10 dB of the main lobe until 20 kHz. The microphones were mounted to a skeletal aluminum frame at the end of 14.75-inch long tubes to approach free field behavior. Acoustic foam, 3.5 inches deep, was attached to the array frame to damp reflections from the frame itself. The array was placed such that the microphone diaphragms were 187 inches from the noise source in the flow-normal direction, and the central microphone of the array was roughly at the same height as the center of the noise source.

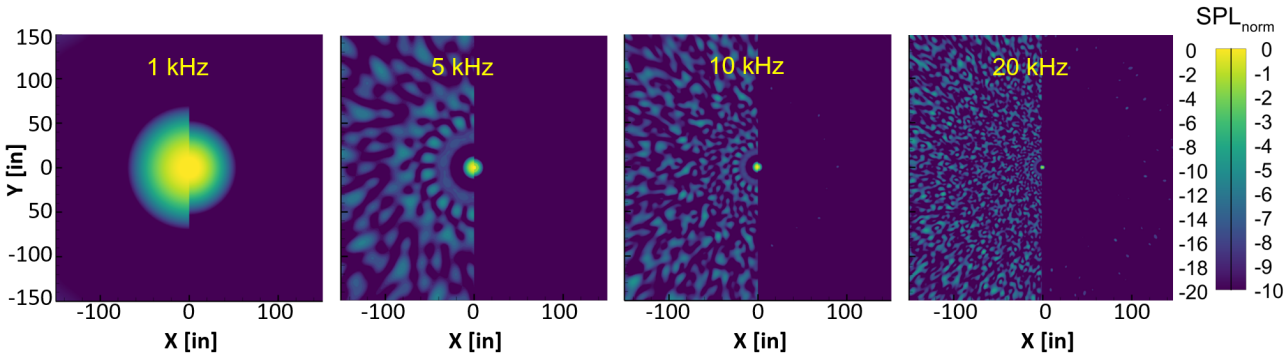

Figure 3: Simulated point spread function of the phased array for a scan grid 187 inches from array.

In addition to the phased array, there was a linear tower array of 11 microphones located opposite the phased array in the test section. These microphones were B&K Type 4939 1/4-inch microphones and sampled at 204,800 samples per second. These microphones were spaced at 1 ft intervals, beginning 28 inches above the test section floor. Both the phased array and the tower array were mounted on traverse rails allowing them to survey various streamwise locations. The traverse rails were programmed to move in parallel such that the center microphones of the two arrays were always directly across from one another. Only the streamwise location in line with the source will be presented in this paper.

2.3. Noise Sources

Two static sources and two inflow sources were used during the test. Source location was kept approximately constant between runs and sources. This was approximately halfway across the test section laterally and 60 inches above the test section floor. To assess reflection and reverberation, high-output speakers were used. A directional noise source was used to more carefully investigate reflective sources in front of and behind the microphone arrays, including the array mounting apparati. The directional source was a Mackie® HR824 cabinet speaker. For the overall reflectivity of the test section, an approximately omnidirectional NTI Audio DS3 Dodecahedron Source speaker was used. Details on static test conditions and reflectivity can be found in the companion paper by Stutz et al. [10]. For noise generation when the tunnel flow was on, noise sources of minimal aerodynamic/aeroacoustic presence were desired. A Dayton Audio DMS58 2” Speaker (Dayton), which had satisfactory output between 300 Hz and 16 kHz, and a high pressure air source (air ball), which produced stochastic broadband noise at frequencies above what the Dayton speaker could achieve, were used. Both inflow noise sources were embedded into a streamlined fairing in the shape

of an ellipse measuring 21 inches in the streamwise direction. The post supporting the noise source was covered with a NACA 0024 airfoil with a 16-inch chord. These aerodynamic treatments were implemented to reduce flow-induced self-noise. An analysis of the air ball source data is beyond the scope of this paper but description of its installation and characterization in a different facility can be found in [11].

3. DATA COLLECTION AND PROCESSING

Data were collected by NI PXIe 449x series dynamic signal acquisition cards installed into a NI PXIe 1085 chassis. Beamforming was carried out using AVEC phased array processing software [12]. Both conventional frequency-domain beamforming (CFDBF) and the CLEAN deconvolution were used. Time-domain data were processed using a Hanning window and 50% overlap between blocks. Frequency resolution used in the computation was 8 Hz; however, the results were re-scaled to 16 Hz for comparison to reference microphone measurements. Reference microphone data were processed using the methods outlined in the companion paper [10].

Scanning grids were defined to cover regions of interest, such as the noise source, inlet, collector, floor, ceiling and wall opposite the phased array (south wall). The scanning grid aligned with the source plane can be seen in Figure 4. AVEC software is able to beamform to grids which are not parallel to the array plane, although the resulting beammaps will be distorted. Processing was able to be carried out on a desktop computer with 32 GB of RAM. To extract spectra from the beammap, a rectangular integration region is defined. The region was sized to contain a 10-dB point spread function for a 1-kHz one-third octave band, which was 100x100 inches for the given source and receiver when axially aligned. The integration region was elongated to accommodate the distortion of the reflected source. Other dynamic ranges were also considered to define the integration region and yielded negligible difference in the resulting spectra.

Static data runs were conducted primarily to assess test section reflectivity and the effectiveness of the acoustic treatments. One significant change was the acoustic treatment on the test section floor, as described by [8]. The acoustic reflectivity of this modified treatment was compared to an acoustically hard surface (plywood) and to an array of acoustic foam wedges.

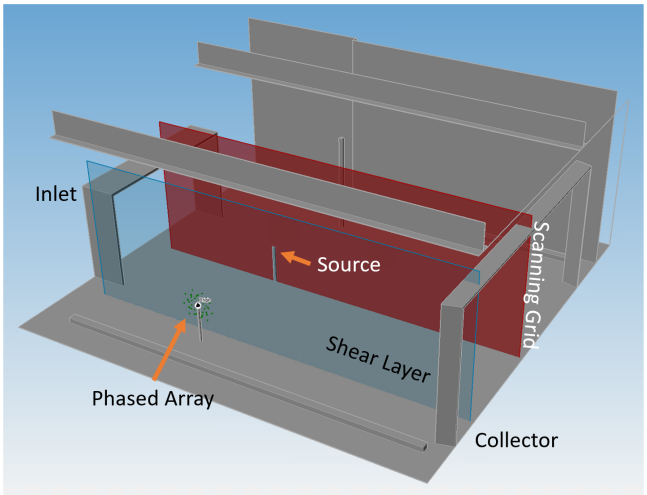

Figure 4: Test section showing scanning grid on source plane and (approximate) shear layer location for given phased array position.

When testing in an open-jet facility, sound waves travelling from the source to the microphone must pass through a shear layer. The changing index of refraction across the shear layer will refract the acoustic waves, thereby changing the propagation path [13]. This may be modeled as an infinitely thin vortex sheet separating a homogeneous core flow and surrounding air [14], which is found to be a reasonable approximation for the flow speeds studied [15]. This model for shear layer correction is employed by the beamforming software to correct for location but does not include amplitude effects, which are assumed to be small for the considered observation angle and Mach

numbers. For a facility the size of the 14x22, the shear layer will typically be turbulent, and acoustic waves will be scattered as well as refracted [16]. This effect of the shear layer on amplitude was not able to be addressed at this time.

Periodic averaging is a useful tool to extract a signal out of random background noise. However, this is only possible when the signal is periodic. When considering propeller or proprotor noise, as was the motivation for the present investigation, tonal noise related to the BPF and its harmonics may be extracted. The application of periodic averaging to data from the present test is discussed in the companion paper [10]. In the case where rotation rate is varying, as is expected to occur with the use of distributed electric propulsors, order tracking schemes such as the Vold-Kalman method can be employed. Pascioni et al. [17] have successfully applied this technique to acoustic data collected from a UAM vehicle. However, when a noise source is aperiodic, self-noise for instance, periodic averaging cannot be leveraged to improve SNR.

4. RESULTS AND DISCUSSION

4.1. Static Runs

Figure 5 shows the CFDBF response of the array for the 1-kHz-centered one-third octave band of a white noise signal from the Mackie speaker. It can be seen that the floor reflection is very clear when considering the acoustically hard plywood (left) but is not discernible over a 10-dB dynamic range when considering the acoustic basket tops alone (right). Reflectivity was also assessed with eight-inch foam wedges placed on the floor between the source and the phased array. There was no meaningful difference found between the reflectivity of the floor baskets alone and with the addition of the foam wedges.

The primary noise sources and reflections from these were integrated to generate the spectra presented in Figure 6. The acoustic baskets (right) can be seen to significantly reduce reflection of mid-frequencies. The sharp dip seen to occur at 1600 kHz in the reflected spectrum for the plywood case (left) is thought to be a result of the speaker directivity, as the reflected spectrum represents sound emitted $\sim 33^\circ$ off of the main axis of the speaker. At frequencies above 10 kHz, the integrated reflection spectrum appears louder than the source spectrum. To the authors' knowledge, this is not physically possible for an unobstructed noise source, and serves as a reminder to interpret such results with care. Beammaps of frequencies above 10 kHz did not exhibit sidelobe levels from the source that were high enough to account for increased levels of the reflection.

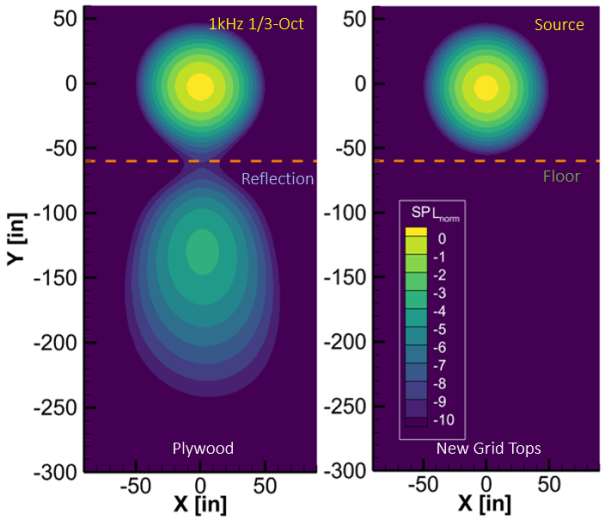

Figure 5: 1-kHz one-third octave band white noise signal from directional source reflecting off plywood (left) and acoustic floor baskets (right).

In the case of acoustic reflection, the frequency response function exhibits characteristic ripples as the primary and reflected noise sources constructively and destructively interfere [18, 19]. Averaging

the spectra over a distribution of microphones, such as a phased array, can mitigate this by providing a range of reflected path lengths, and thus, the pattern of interference is smoothed. The benefit of simple averaging is that it is computationally simple compared to beamforming. However, simple averaging cannot help localize a noise source in space. Additionally, simple averaging will incorporate power from the reflected source, which may result in an artificially higher overall noise level. The characteristic ripple in the reference microphone spectrum can be seen in the left panel of Figure 6. It can also be seen that in the presence of a reflective surface, the average sound pressure level is higher than the integrated level. Whereas when the reflective surface is removed, as can be seen in the right panel of Figure 6, the averaged level is much closer to the integrated level. This suggests that the reflected random signal is, on net, adding to the acoustic energy received by the microphones [18], but that integrating around the source rejects that contribution.

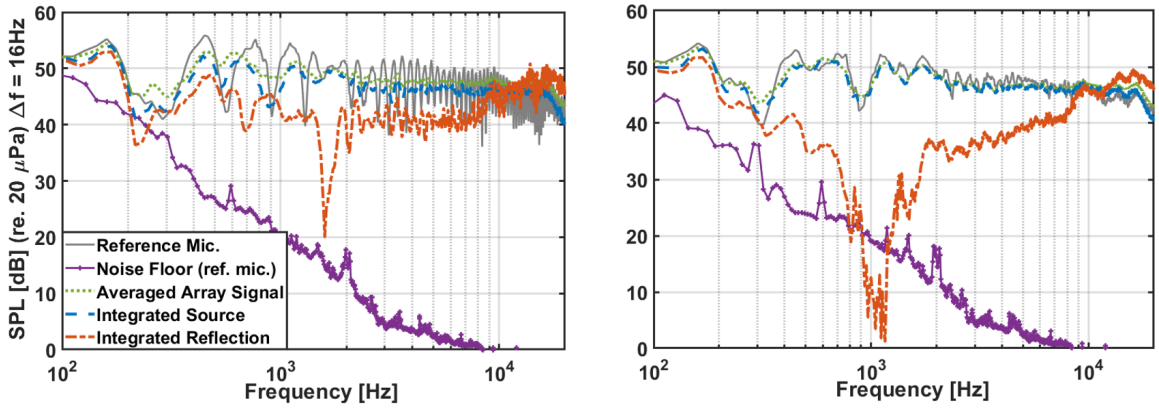

Figure 6: Aperiodic band-limited white noise over plywood (left) and acoustic floor baskets (right).

4.2. Flow-on Runs

Perhaps a larger acoustic concern than reflectivity in the test section is the flow noise. Empty test section measurements were taken at all flow speeds and examined using the reference microphone at the center of the phased array. Figure 7 shows the narrowband spectra of the tunnel background noise from Mach 0.00 (static) to Mach 0.16. As flow speed is increased, significant flow noise is added for all frequencies investigated.

Operating in the open-jet configuration, the source noise must cross a shear layer to reach out-of-flow microphones. Figure 8 shows the effect of the shear layer turbulence on the propagation and analysis of acoustic signals, and how periodic averaging and phased array processing can improve SNR in different frequency domains. The upper-left panel shows the results of CFDBF for a periodic multisine waveform from 300 Hz to 10 kHz, measured with no flow and through the shear layer at Mach 0.06, 0.08 and 0.12. At low frequencies the phased array struggles to isolate the noise source in the integration region, and so frequencies below 1 kHz cannot be fully separated from the flow noise. This is not surprising as the array was designed to resolve frequencies between 1 kHz and 16 kHz. At higher frequencies, approaching the upper threshold of the output signal, the phased array is able to track the signal. At 10 kHz the difference between the static signal and the Mach 0.12 case is 5 dB. Recall that the shear layer correction applied only addresses source location, not the amplitude. The upper-right, lower-left and lower-right panels compare integrated phased array spectra to periodically averaged spectra at Mach 0.06, 0.08 and 0.12, respectively. The flow-off integrated phased array response (solid black line) and the unprocessed signal from the reference microphone (dashed grey

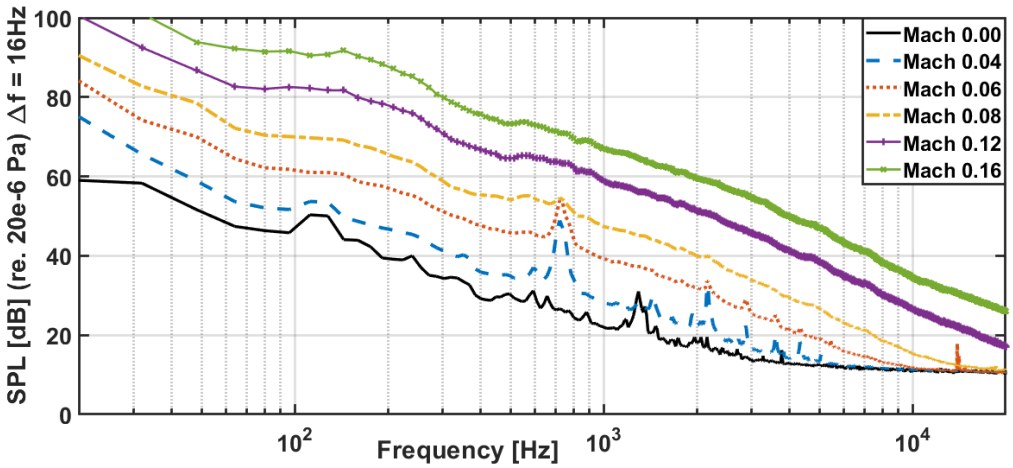

Figure 7: Tunnel background noise as a function of Mach number for the empty test section, measured by the reference microphone.

line) are included for comparison. It can be seen that at the Mach 0.06 flow speed, periodic averaging of the reference microphone data successfully recovers the low frequencies in the acoustic signal but is already struggling to resolve the high end. The performance of periodic averaging continues to degrade compared to beamforming at high frequencies as the freestream Mach number increases. Periodic averaging also degrades at low frequencies as Mach number increases, but still suppresses background noise better than the phased array. As discussed in [10], amplitude and phase distortion by the shear layer increases with increasing flow speeds, and is more significant for higher frequencies. At the highest flow speed, the difference between the static signal and periodically averaged signal rises to 16 dB at 10 kHz. At the onset of the static signal, which will be taken to be closer to 350 Hz than 300 Hz, the beamformed signal exceeds the static by 16 dB, whereas the periodically averaged signal exceeds the static by 6 dB. However, the beamformed signal is substantially below the unprocessed reference level, indicating that beamforming is reducing background noise but not suppressing it entirely.

Figure 9 shows the same frequency range and approximate acoustic output as Figure 8, except that in this case the signal is random white noise with no period to average over. It may again be observed that the phased array can follow the signal at high frequencies with reasonable fidelity, although beamformed results above 8 kHz better track the unprocessed reference signal than the static result, particularly for the Mach 0.08 and 0.12 flow speeds. Recall the processing software does not account for deterministic attenuation by the shear layer or scattering by its turbulence. Also, as before, low frequency background noise is effectively rejected while frequencies are within the optimal working range of the array.

The reader will notice a prominent dip in the spectra occurring ~1450 Hz in Figures 8 and 9 for all flow speeds, including static. Rather than a directivity effect, as was seen in §4.1 with the Mackie speaker, this is likely an installation effect. The Dayton speaker is recessed into a shallow circular cavity with diameter ranging from 9.75 inches to 10.75 inches. Given the atmospheric conditions in the test cell at the time, such a cavity size can be expected to produce a null between 1285 and 1425 Hz. The cause of the null present at 890 Hz, seen most prominently in the Mach 0.12 flow, has not been determined.

Acoustic beamforming can help determine the sources of background noise. For instance, the

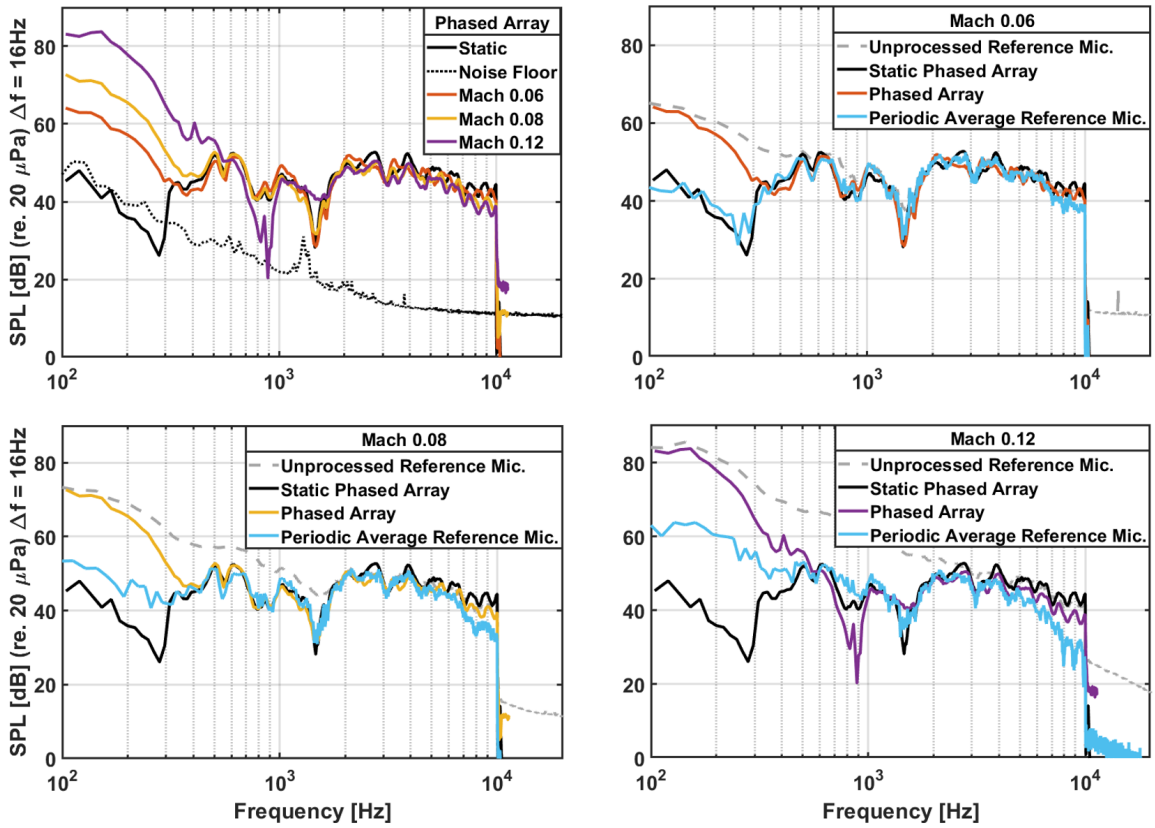

Figure 8: Periodic multisine wave signal processed using CFDBF and periodic averaging to address low SNR caused by high flow noise.

upper panel of Figure 10 shows the narrowband at which the 2160 Hz tone seen in Figure 7 occurs for Mach 0.04 flow. One can see that a source in the direction of the collector is the most prominent source of this tone. At a slightly higher frequency the noise source from the collector can no longer be seen, as shown in the lower panel. This tone was later determined to likely originate from the facility fan drive motor cooling unit, the strongest peak from this source occurring at 720 Hz. The fan and cooling unit are roughly opposite the test section in tunnel circuit, but there are significantly fewer flow conditioning treatments and obstructions downstream of the test section than upstream, so it is reasonable that the tone is more noticeable from that direction. A schematic of the 14x22 circuit can be found in [4]. The stronger peak at 720 Hz was not assessed through beamforming due to that frequency being outside the optimal range of the array. This tone and its associated harmonics were also observed in the background acoustic spectra from the Common Research Model Test carried out in the 14x22 in 2021.

4.3. Deconvolution

So far, the results presented have been generated using CFDBF. Integration around sources on the map yields reasonably quantitative results when the source is directly facing the array and the integration region is centered around the main source. If one or both of these conditions is not met, the resulting spectra will be inaccurate. For instance, integrating a beammap of a reflection will return a spectrum; however, the results may be misleading, as pointed out for Figure 6. The deconvolution algorithm CLEAN can be applied to reduce this discrepancy. Although the reflection is not the dominant noise

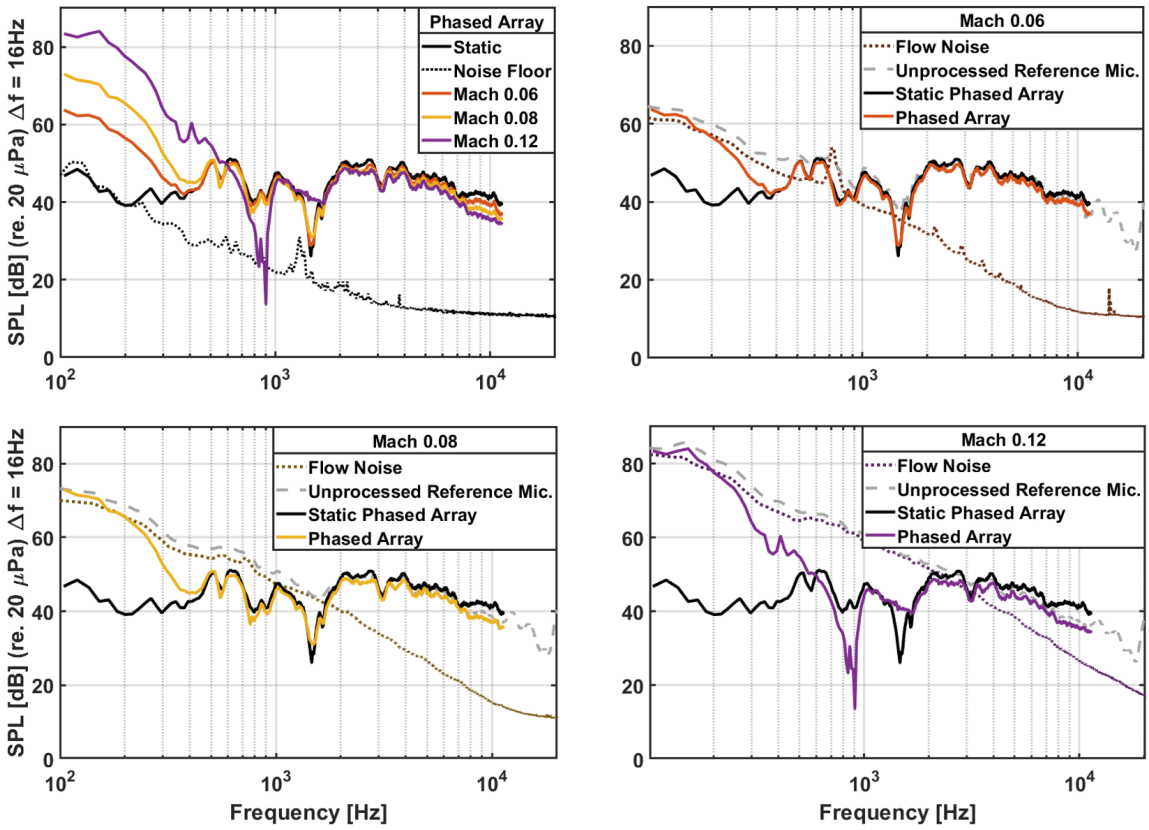

Figure 9: Aperiodic band-limited white noise signal processed using conventional frequency domain beamforming.

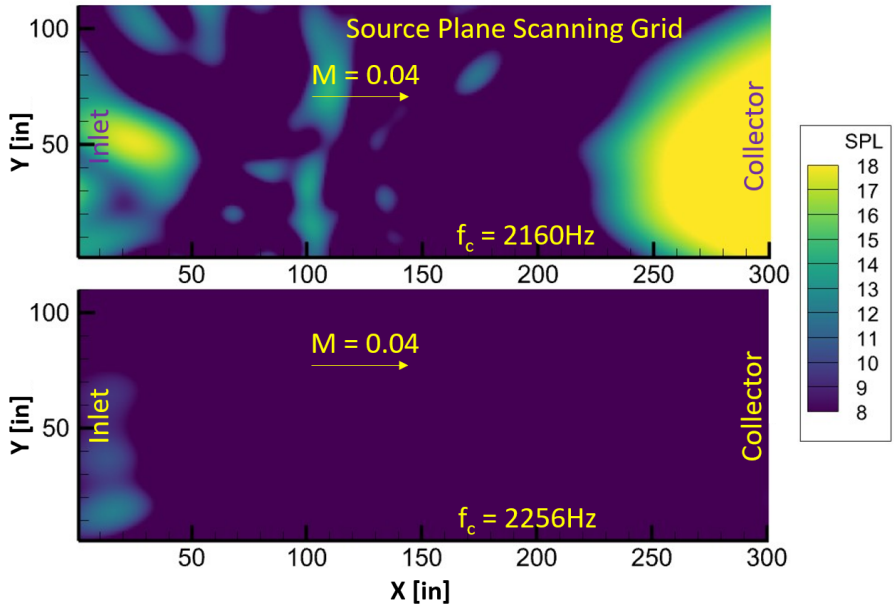

Figure 10: Mid plane of tunnel test-section at Mach 0.04 freestream. Narrowband beammap centered at 2160 Hz (upper); narrowband beammap centered on 2256 Hz (lower).

source in the domain, it is sufficiently well separated from the dominant source that CLEAN is an

appropriate choice. This can be seen in Figure 11 where CLEAN results are compared to conventional integrated spectra for white noise over a reflective surface. The veracity of these results may still be uncertain as it is inherently difficult to directly measure a reflection.

Applying CLEAN as a post-processing step to a signal passing through the shear layer improved performance below the design frequency of the phased array, but also reduced amplitude at higher frequencies where CFDBF worked well. For the sake of brevity, only the static and Mach 0.12 cases are presented for the multisine waveform in Figure 12 to demonstrate this point. It can be seen in both the left and the right panels that CLEAN suppresses background noise better than CFDBF in both flow states at low frequencies. However, CLEAN is particularly sensitive to the effects of decorrelation. As shown in the right panel of Figure 12, CFDBF outperforms CLEAN in capturing higher frequency content when a shear layer is present.

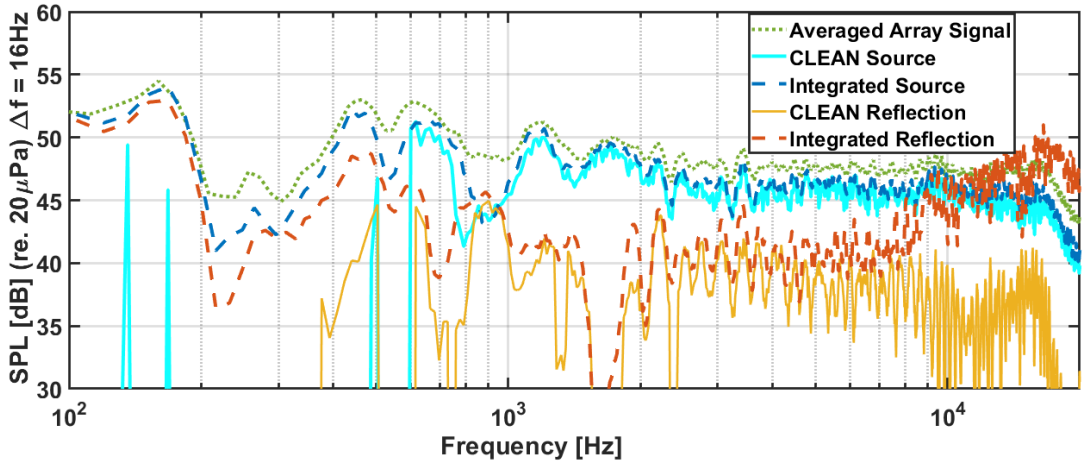

Figure 11: Primary source and reflected source calculated through CFDBF and CLEAN for an aperiodic band-limited white noise source.

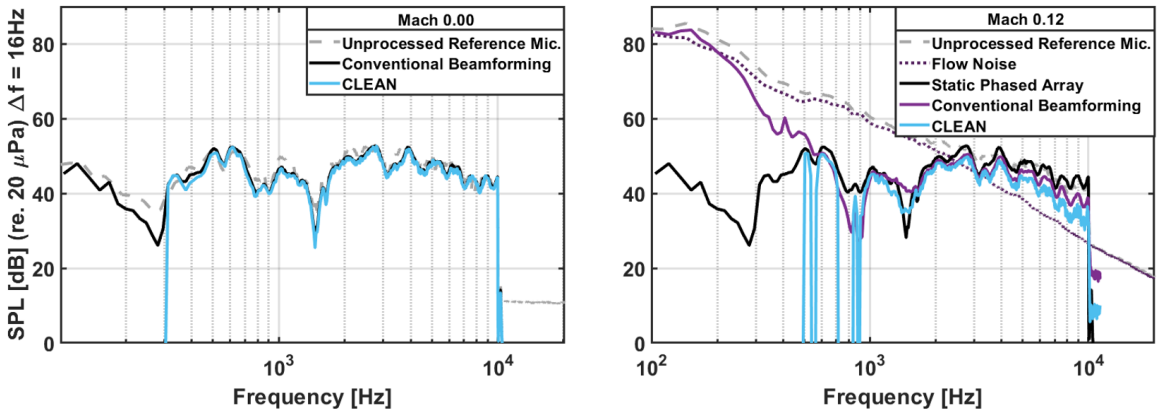

Figure 12: Periodic multisine waveform signal calculated through CFDBF and CLEAN.

5. CONCLUSIONS

This test performed with known acoustic sources will allow better interpretation of results when the source itself is the topic of investigation. The modifications to the acoustic floor treatment in the

NASA Langley Research Center 14- by 22-Foot Subsonic Tunnel reduced floor reflections to a level indistinguishable from an acoustic wedge treatment. When reflections are present, single-microphone methods will overestimate the total level, and simple averaging across several microphones will smooth reflection ripples but not correct the overestimation. Integrating the beammap around the source effectively rejects the acoustic contribution of the reflections.

The phased array is superior to single-microphone periodic averaging for high frequency noise passing through a turbulent shear layer. At frequencies below the array's optimized range, periodic averaging is superior for extracting signal content. However, beamforming can still reduce background noise at those frequencies and so is helpful when the source under investigation is random. Application of the CLEAN deconvolution algorithm also improves the low frequency performance for both static and flow-on cases. When flow is present, CFDBF better captures the high frequency content.

ACKNOWLEDGMENTS

The authors would like to acknowledge the hard work of the LSAWT and the 14x22 technicians and engineers, as well as Matthew Galles for his help with designing the new floor treatment.

REFERENCES

[1] F. V. Hutcheson, D. P. Lockard, and D. Stead. On the alleviation of background noise for the High-Lift Common Research Model aeroacoustic test. In *28th AIAA/CEAS Aeroacoustics Conference*, AIAA Paper 2022-2988, Southampton, UK, June 2022.

[2] W. M. Humphreys, D. P. Lockard, and C. J. Bahr. Characterization of slat noise radiation from a high-lift common research model. *AIAA Journal*, 61(10):4556–4578, October 2023.

[3] S. L. Heath, T. F. Brooks, F. V. Hutcheson, M. J. Doty, H. H. Haskin, T. Spalt, C. J. Bahr, C. L. Burley, S. Bartram, W. Humphreys, C. Lunsford, T. Popernack, S. Colbert, D. Hoad, L. Becker, D. Stead, D. Kuchta, and L. Yeh. Hybrid Wing Body aircraft acoustic test preparations and facility upgrades. In *28th AIAA Aerodynamic Measurement Technology, Ground Testing, and Flight Testing Conference*, AIAA Paper 2013-2623, San Diego, CA, 2013.

[4] S. L. Heath, T. F. Brooks, F. V. Hutcheson, M. J. Doty, C. J. Bahr, D. Hoad, L. Becker, W. M. Humphreys, C. L. Burley, D. Stead, D. S. Pope, T. B. Spalt, D. H. Kuchta, G. E. Plassman, and J. A. Moen. NASA Hybrid Wing Body aircraft aeroacoustic test documentation report. Technical Report TM–2016-219185, National Aeronautics and Space Administration, 2016.

[5] M. R. Khorrami, W. M. Humphreys, and D. P. Lockard. An assessment of flap and main landing gear noise abatement concepts. In *21st AIAA/CEAS Aeroacoustics Conference*, AIAA Paper 2015-2987, Dallas, TX, June 2015.

[6] M. J. Doty, T. F. Brooks, C. L. Burley, C. J. Bahr, and D. S. Pope. Jet noise shielding provided by a Hybrid Wing Body aircraft. In *20th AIAA/CEAS Aeroacoustics Conference*, AIAA Paper 2014-2625, Atlanta, GA. June 2014.

[7] M. A. Marcolini, D. A. Conner, J. T. Brieger, L. E. Becker, and C. D. Smith. Noise characteristics of a model tiltrotor. In *American Helicopter Society's 51st Annual Forum and Technology Display*, Fort Worth, TX, May 1995.

[8] N. S. Zawodny, K. A. Pascioni, A. H. Lind, M. B. Galles, C. M. Stutz, and M. L. Houston. Reflectivity characterization of in-flow acoustic floor treatment for the NASA Langley 14- by 22-Foot Subsonic Tunnel. Submitted for publication to *53rd International Congress and Exposition on Noise Control Engineering*, Nantes, France, August 2024.

[9] R. Reger, N. S. Zawodny, K. Pascioni, D. Wetzel, F. Liu, and L. N. Cattafesta. Design-optimization of a broadband phased microphone array for aeroacoustic application. In *Acoustical Society of America Meeting*, Hong Kong, China, May 2012.

[10] C. M. Stutz, M. L. Houston, N. S. Zawodny, and K. A. Pascioni. Acoustic characterization of the NASA Langley 14- by 22-Foot Subsonic Tunnel using single-microphone analysis techniques. In *Noise-Con 2024*, New Orleans, LA, June 2024.

[11] C. Horne and N. Burnside. Initial calibrations and wind tunnel test results for an in-flow reference array using new in-flow acoustic sources in four array mount configurations. In *Proceeding of AIAA Aviation 2018*, AIAA Paper 2018-2969, Atlanta, GA, June 2018.

[12] Acoustical Vibrations Engineering Consultants Inc. *Phased Array Software Version 5.15 User Manual*, 2022. www.avec-engineering.com.

[13] T. J. Mueller. *Aeroacoustic Measurements*. Springer Science & Business Media, 2002.

[14] R. K. Amiet. Correction of open jet wind tunnel measurements for shear layer refraction. In *Second Aeroacoustics Conference*, AIAA Paper 75-532, Hampton, VA, March 1975.

[15] R. K. Amiet. Refraction of sound by a shear layer. *Journal of Sound and Vibration*, 58:467–482, 1978.

[16] K. K. Ahuja, H. K. Tanna, and B. J. Tester. An experimental study of transmission, reflection and scattering of sound in a free jet flight simulation facility and comparison with theory. *Journal of Sound and Vibration*, 75:51–85, 1981.

[17] K. A. Pascioni, J. Bain, and A. Thai. Propeller source noise separation from flight test measurements of the Joby Aviation aircraft. Submitted for publication to *30th AIAA/CEAS Aeroacoustics Conference*, Rome, Italy, June 2024.

[18] E. M. Salomons. *Computational Atmospheric Acoustics*. Springer Dordrecht, 2001.

[19] B. N. Shivashankara and G. W. Stubbs. Ground plane microphone for measurement of aircraft flyover noise. *Journal of Aircraft*, 24:751–758, 1987.